Latin American Journal of Solids and Structures
www.lajss.org

Nonlinear Electromechanical Stability of a Functionally Graded Circular Plate Integrated With Functionally Graded Piezoelectric Layers

Abstract

This research develops nonlinear electromechanical stability of a circular functionally graded plate integrated with functionally graded piezoelectric layers under compressive radial force. Geometric nonlinearity is considered in the strain-displacement relation using Von-Karman relation. The structure is loaded under mechanical and electrical loads. Distribution of electric potential is considered along the radial and thickness direction. The top and bottom of both piezoelectric layers is short-circuited. The effect of various values of non homogenous index for both functionally graded (FG) and functionally graded piezoelectric (FGP) layers can be considered on the responses of the system. Furthermore, a comprehensive study for evaluation of geometric parameters can be performed on the critical loads of the structure.

Keywords

Stability, functionally graded piezoelectric, circular plate, nonlinearity, functionally graded materials

Mohammad Arefi [a]

[a] Department of Solid Mechanic, Faculty of Mechanical Engineering, University of Kashan, Kashan, Iran, 87317-51167.
E-mail: Arefi63@gmail.com
arefi@kashanu.ac.ir

http://dx.doi.org/10.1590/1679-78251449

Received 07.07.2014
In Revised Form 31.01.2015
Accepted 17.02.2015
Available online 19.02.2015

1 INTRODUCTION

Functionally graded materials have been produced for usage in environment with opposite conditions. Opposite conditions means such environment that needs two or more properties for covering all requirements. For example, some researchers have tried to create a material that is applicable in spacecrafts. As we know, the temperature of spacecraft body at outer layers is very high while the temperature at inner layers is not very high. For these conditions, the researchers provide some innovative materials with variable properties.

For example a combination of ceramic and metal can be used as functionally graded materials. The material properties are changed gradually from metal to ceramic. This change may be described by a function along the thickness or other dimension of the structure. Composition of functionally graded materials with piezoelectric elements proposes new intelligent materials that can be studied in this paper. The piezoelectric effect has been presented scientifically by Pierre and Jacques Curie in 1880. Piezoelectric structures are very applicable in the industrial systems as sensor or actuator in various geometries such as plates, cylinders and shells. In order to control the distribution of the displacement or electric potential in a piezoelectric structure, functionally graded piezoelectric material (FGPM) can be used. An investigation on the literature can justifies necessity of this research.

Wu et al. (2002) have used GDQR (generalized differential quadrature rule) for free vibration analysis of solid circular plates. O¨ zakc et al. (2003) have focused on the buckling load optimization of variable thickness circular and annular plates using finite element approach. Ma and Wang (2003) have presented deflection bending of a functionally graded circular plate using the classical nonlinear von Karman plate theory. The plate has been subjected to various types of loading such as mechanical and thermal loadings. As the results of that study, nonlinear bending and critical buckling temperature and thermal post-buckling behavior of the FGM plates were discussed. The stability of parametric vibrations of circular plate subjected to in-plane forces was analyzed using the Liapunov method by Tylikowski and Frischmuth (2003).

Zhou et al. (2003) employed Chebyshev–Ritz method in three-dimensional free vibration analysis of circular and annular plates. They used a linear analysis with small strain assumption. Based on the geometric properties of circular and annular plates, the vibration was divided into three distinct categories: axisymmetric vibration, torsional vibration and circumferential vibration. Li et al. (2004) used a large deflection bending analysis of an axisymmetric simply supported circular plate. The incremental load technique was developed for solving the bending problem of a thin circular plate with large deflection. They have found that the employed technique has capability in solution of engineering problems. A circular plate containing piezoelectric layers as actuator under static and dynamic mechanical and electrical loads and using Kirchhoff plate model have been sudied by Sekouri et al. (2004). Experiments using a thin circular aluminum plate structure with distributed piezoelectric actuators were also conducted to verify the analysis and the computer simulations.

Kang et al. (2005) presented a closed form solution for finding the natural frequencies and mode shapes of a circular orthotropic plate using Rayleigh–Ritz method. They have found that the obtained results have capability in designing of circular plates such as wood disk as an orthotropic composite material.

Nosier and Fallah (2009) studied axisymmetric and asymmetric behavior of functionally graded circular plates under transverse mechanical loading using the first-order shear deformation plate theory with von Karman non-linearity. By introducing a stress function and a potential function, the problem were uncoupled to form equations describing the interior and edge-zone problems of FG plates. A perturbation technique, in conjunction with Fourier series method to model the problem asymmetries, is used to obtain the solution for various clamped and simply supported boundary conditions. Camier et al. (2009) studied Large-amplitude and geometrically

nonlinear vibrations of free-edge circular plates with geometric imperfections. Free vibration analysis of circular thin plate with three types of boundary conditions have been studied by Yalcin et al. (2009). The solution procedure has been performed using differential transform method. The obtained results using this semi-numerical–analytical solution technique have been compared with results of Bessel function solution. Axisymmetric bending and buckling of perfect functionally graded solid circular plates have been studied by Saidi et al. (2009) based on the unconstrained third-order shear deformation plate theory (UTST). The obtained results have been compared with those results extracted using lower order shear deformation theories. Sahraee and Saidi (2009) investigated axisymmetric bending and stretching of functionally graded (FG) circular plates subjected to uniform transverse loading based on fourth-order shear deformation plate theory (FOST). Gradation of used material has been considered along the thickness direction based on a power law function. Vivio and Vullo (2010) introduced a new analytical method for evaluation of elastic stresses and deformations in the solid and annular circular plates with variable thickness subjected to transverse loading. Arefi (2013) and Arefi and Nahas (2014) presented nonlinear analysis of the functionally graded piezoelectric cylinder and sphere, respectively. Three dimensional analysis of a functionally graded piezoelectric shell under multi fields has been studied by Arefi (2014).

An investigation on the literature indicates that there is no published work to study the nonlinear electromechanical stability of a functionally graded circular plate integrated with functionally graded piezoelectric materials under mechanical and electrical loads. Some useful information about linear and nonlinear analysis of functionally graded piezoelectric materials can be considered in the literature [Asemi et al. 2014, Arefi and Rahimi 2011, Arefi and Rahimi 2012 (a, b, c, d, e, f), Rahimi et al, 2011, Khoshgoftar et al, 2009].

2 FORMULATION

Fundamental equations for mechanical stability of the functionally graded plates integrated with two functionally graded piezoelectric layers at top and bottom of plate is developed in the present section. Classical plate theory (CPT) is used for simulation of deformation components of the plate. r,θ,z is used for components of coordinate system and u,w is used for symmetric components of plate deformation. Based on the above assumptions, the deformation components can be given as follows: [Arefi and Rahimi, 2012]

$$\begin{cases} u(r,z) = u_0(r) - z\,\dfrac{\partial w_0(r)}{\partial r} \\ w(r,z) = w_0(r) \end{cases} \tag{1}$$

The strain components can be derived from nonlinear strain-displacement relation (Von-Karman) [Arefi and Rahimi, 2012]

$$\{\varepsilon\} = \frac{1}{2}\left\{\nabla\vec{u} + \nabla\vec{u}^{T} + (\nabla\vec{u})^{T}(\nabla\vec{u})\right\} \tag{2}$$

Using above relation, three in-plane components of strain can be obtained as follows:

$$\begin{aligned}
\varepsilon_{rr} &= \frac{\partial u_0}{\partial r} - z\frac{\partial^2 w_0}{\partial r^2} + \frac{1}{2}\left(\frac{\partial w}{\partial r}\right)^2 = \varepsilon_{rm} + z\,\kappa_r \\
\varepsilon_{\theta\theta} &= \frac{u_0}{r} - \frac{z}{r}\frac{\partial w_0}{\partial r} = \varepsilon_{\theta m} + z\,\kappa_\theta \\
\varepsilon_{rz} &= \frac{\partial u}{\partial z} + \frac{\partial w}{\partial r} = -\frac{\partial w_0(r)}{\partial r} + \frac{\partial w_0(r)}{\partial r} = 0
\end{aligned} \tag{3}$$

The simplified notation can be shown as follows:

$$\begin{aligned}
\varepsilon_{rm} &= \frac{\partial u_0}{\partial r} + \frac{1}{2}\left(\frac{\partial w}{\partial r}\right)^2, \kappa_r = -\frac{\partial^2 w_0}{\partial r^2} \\
\varepsilon_{\theta m} &= \frac{u_0}{r}, \kappa_\theta = -\frac{1}{r}\frac{\partial w_0}{\partial r}
\end{aligned} \tag{4}$$

After determination of strain components, the constitutive equations can be separately derived for both functionally graded and functionally graded piezoelectric layers. These equations for functionally graded layer are: [Arefi and Rahimi, 2012; Gaur and Rana, 2014]

$$\begin{cases}
\sigma^e{}_{rr} = \dfrac{E}{1-\nu^2}\{\varepsilon_{rr} + \nu\varepsilon_{\theta\theta}\} = \dfrac{E}{1-\nu^2}\{\varepsilon_{rm} + z\,\kappa_r + \nu(\varepsilon_{\theta m} + z\,\kappa_\theta)\} \\
\sigma^e{}_{\theta\theta} = \dfrac{E}{1-\nu^2}\{\varepsilon_{\theta m} + z\,\kappa_\theta + \nu(\varepsilon_{rm} + z\,\kappa_r)\}
\end{cases} \tag{5}$$

And for functionally graded piezoelectric layers are: [Arefi and Rahimi, 2012]

$$\begin{cases}
\sigma_{rr} = C^p{}_{rrrr}\varepsilon_{rr} + C^p{}_{rr\theta\theta}\varepsilon_{\theta\theta} - e_{rrr}E_r - e_{rrz}E_z \\
\sigma_{\theta\theta} = C^p{}_{\theta\theta rr}\varepsilon_{rr} + C^p{}_{\theta\theta\theta\theta}\varepsilon_{\theta\theta} - e_{\theta\theta r}E_r - e_{\theta\theta z}E_z
\end{cases} \tag{6}$$

In order to complete the constitutive relations, in this step, the electric potential distribution must be defined. A three dimensional distribution of electric potential can be represented as multiplication of two functions one through radial direction $\phi(r)$ and another through thickness direction $f(z)$.

$$\phi(r,z) = \phi(r)f(z) \tag{7}$$

where, $f(z)$ must satisfy electric potential boundary conditions along the thickness (transverse) direction. The short-circuited boundary conditions is considered for both top and bottom piezoelectric layers. By employing a second order approximation for electric potential distribution along the z direction, we'll have: [Ebrahimi and Rastgo, 2008]

$$\phi(r,z) = \phi f = \phi(r)\{1 - (\frac{2z - 2h_e - h_p}{h_p})^2\} \tag{8}$$

Using the above equation, the electric filed components can be derived as follows:

$$\phi(r,z)=\phi f \ \rightarrow E_k=-\frac{\partial\phi(r,z)}{\partial x_k}, x_k=r,z \ \rightarrow$$
$$\begin{cases} E_r=-\dfrac{\partial\phi(r,z)}{\partial r}=-f\ \phi_{,r} \\ E_z=-\dfrac{\partial\phi(x,y,z)}{\partial z}=-f_{,z}\,\phi \end{cases} \tag{9}$$

By substitution of electric field components from Eq. (9) into constitutive equations of piezoelectric layers (Eq. (6)), we will have:

$$\begin{cases} \sigma_{rr}=C^p{}_{rrrr}(\varepsilon_{rm}+z\kappa_r)+C^p{}_{rr\theta\theta}(\varepsilon_{\theta m}+z\kappa_\theta)+e_{rrr}f\phi_{,r}+e_{rrz}f_{,z}\phi \\ \sigma_{\theta\theta}=C^p{}_{\theta\theta rr}(\varepsilon_{rm}+z\kappa_r)+C^p{}_{\theta\theta\theta\theta}(\varepsilon_{\theta m}+z\kappa_\theta)+e_{\theta\theta r}f\phi_{,r}+e_{\theta\theta z}f_{,z}\phi \end{cases} \tag{10}$$

In order to attain the final governing equations, the resultant of force and moments per unit width must be evaluated.

$$\begin{cases} N_{ij}=\int_{-(h_e+h_p)}^{(h_e+h_p)}\sigma_{ij}dz \\ M_{ij}=\int_{-(h_e+h_p)}^{(h_e+h_p)}\sigma_{ij}zdz \end{cases}, ij=rr,\theta\theta \tag{11}$$

As mentioned above, the integral must be evaluated along the thickness direction. Since the plate is included two different materials, above integral must be decomposed into two integral

$$\begin{aligned} N_{ij}&=\int_{-(h_e+h_p)}^{(h_e+h_p)}\sigma_{ij}dz=\int_{-h_e}^{h_e}\sigma^e{}_{ij}dz+2\int_{h_e}^{h_e+h_p}\sigma^p{}_{ij}dz \\ M_{ij}&=\int_{-(h_e+h_p)}^{(h_e+h_p)}\sigma_{ij}z\,dz=\int_{-h_e}^{h_e}\sigma^e{}_{ij}z\,dz+2\int_{h_e}^{h_e+h_p}\sigma^p{}_{ij}z\,dz \end{aligned} \tag{12}$$

Substituting the stress relations in terms of strain components and electric potential presents the resultant of force and moments as follows:

$$\begin{aligned} N_{rr}&=\frac{E_1}{1-\nu^2}\{\varepsilon_{rm}+\nu\varepsilon_{\theta m}\}+\frac{E_2}{1-\nu^2}\{\kappa_r+\nu\kappa_{\theta\theta}\}+A_1\varepsilon_{rm}+A_2\kappa_r+A_3\varepsilon_{\theta m}+A_4\kappa_\theta+A_5\phi_{,r}+A_6\phi \\ N_{\theta\theta}&=\frac{E_1}{1-\nu^2}\{\varepsilon_{\theta m}+\nu\varepsilon_{rm}\}+\frac{E_2}{1-\nu^2}\{\kappa_\theta+\nu\kappa_r\}+A_3\varepsilon_{rm}+A_4\kappa_r+A_7\varepsilon_{\theta m}+A_8\kappa_\theta+A_9\phi_{,r}+A_{10}\phi \\ M_{rr}&=\frac{E_2}{1-\nu^2}\{\varepsilon_{rm}+\nu\varepsilon_{\theta m}\}+\frac{E_3}{1-\nu^2}\{\kappa_r+\nu\kappa_\theta\}+A_2\varepsilon_{rm}+A_{11}\kappa_r+A_4\varepsilon_{\theta m}+A_{12}\kappa_\theta+A_{13}\phi_{,r}+A_{14}\phi \\ M_{\theta\theta}&=\frac{E_2}{1-\nu^2}\{\varepsilon_{\theta m}+\nu\varepsilon_{rm}\}+\frac{E_3}{1-\nu^2}\{\kappa_\theta+\nu\kappa_r\}+A_4\varepsilon_{rm}+A_{15}\kappa_r+A_8\varepsilon_{\theta m}+A_{16}\kappa_\theta+A_{17}\phi_{,r}+A_{18}\phi \end{aligned} \tag{13}$$

where, mentioned coefficients E_i, A_i may be considered in Appendix A.

Defined components of the resultant of force and moments must satisfy equilibrium equations as follows:

$$\begin{cases} \dfrac{\partial N_{rr}}{\partial r}+\dfrac{N_{rr}-N_{\theta\theta}}{r}=0 \\ \dfrac{\partial M_{rr}}{\partial r}+\dfrac{M_{rr}-M_{\theta\theta}}{r}-rF_{r,cr}\left(\dfrac{\partial^2 w}{\partial r^2}+\dfrac{1}{r}\dfrac{\partial w}{\partial r}\right)=0 \end{cases} \tag{14}$$

Substitution of resultant of force and moments in equilibrium equations yields:

$$\begin{aligned} &\frac{E_1}{1-\nu^2}\{\varepsilon_{rm,r}+\nu\varepsilon_{\theta m,r}\}+\frac{E_2}{1-\nu^2}\{\kappa_{rr,r}+\nu\kappa_{\theta\theta,r}\}+A_1\varepsilon_{rm,r}+A_2\kappa_{rr,r}+A_3\varepsilon_{\theta m,r}+A_4\kappa_{\theta\theta,r}+A_5\phi_{,rr}+A_6\phi_{,r} \\ &\frac{E_1}{r(1+\nu)}\{\varepsilon_{rm}+\varepsilon_{\theta m}\}+\frac{E_2}{r(1+\nu)}\{\kappa_{rr}+\kappa_{\theta\theta}\}+\{A_1-A_3\}\frac{\varepsilon_{rm}}{r}+\{A_2-A_4\}\frac{\kappa_{rr}}{r}+\{A_3-A_7\}\frac{\varepsilon_{\theta m}}{r}+\{A_4-A_8\}\frac{\kappa_{\theta\theta}}{r} \\ &+\{A_5-A_9\}\frac{\phi_{,r}}{r}+\{A_6-A_{10}\}\frac{\phi}{r}=0 \end{aligned}$$

$$\begin{aligned} &\frac{E_2}{1-\nu^2}\{\varepsilon_{rm,r}+\nu\varepsilon_{\theta m,r}\}+\frac{E_3}{1-\nu^2}\{\kappa_{r,r}+\nu\kappa_{\theta,r}\}+A_2\varepsilon_{rm,r}+A_{11}\kappa_{r,r}+A_4\varepsilon_{\theta m,r}+A_{12}\kappa_{\theta,r}+A_{13}\phi_{,rr}+A_{14}\phi_{,r} \\ &\frac{E_2}{r(1+\nu)}\{\varepsilon_{rm}+\varepsilon_{\theta m}\}+\frac{E_3}{r(1+\nu)}\{\kappa_{r}+\kappa_{\theta}\}+\{A_2-A_4\}\frac{\varepsilon_{rm}}{r}+\{A_{11}-A_{15}\}\frac{\kappa_{r}}{r}+\{A_4-A_8\}\frac{\varepsilon_{\theta m}}{r}+\{A_{12}-A_{16}\}\frac{\kappa_{\theta}}{r} \\ &+\{A_{13}-A_{17}\}\frac{\phi_{,r}}{r}+\{A_{14}-A_{18}\}\frac{\phi}{r}-rF_{r,cr}\left(\frac{\partial^2 w}{\partial r^2}+\frac{1}{r}\frac{\partial w}{\partial r}\right)=0 \end{aligned} \tag{15}$$

Electric displacement equations along the three directions are [Gaur and Rana, 2014]:

$$\begin{cases} D_r=e_{rrr}(\varepsilon_{rm}+z\,\kappa_r)+e_{r\theta\theta}(\varepsilon_{\theta m}+z\,\kappa_\theta)-\eta_{rr}\phi_{,r}f\ -\eta_{rz}\phi_{,z}f \\ D_z=e_{zrr}(\varepsilon_{rm}+z\,\kappa_r)+e_{z\theta\theta}(\varepsilon_{\theta m}+z\,\kappa_\theta)-\eta_{zr}\phi_{,r}f\ -\eta_{zz}\phi f_{,z} \end{cases} \tag{16}$$

Discharge equation that implies divergence of electric displacement vanishes through the piezoelectric section yields third equation as follows: [Ebrahimi and Rastgo, 2008]

$$\int_{h_e}^{h_e+h_p}(\vec{\nabla}.\vec{D})dz=\int_{h_e}^{h_e+h_p}\left(\frac{\partial D_r}{\partial r}+\frac{D_r}{r}+\frac{\partial D_z}{\partial z}\right)dz \tag{17}$$

Substitution of electric displacement equations into discharge equation yields:

$$\begin{aligned} &A_{19}\{\varepsilon_{rm,r}+\frac{\varepsilon_{rm}}{r}\}+A_{20}\{\kappa_{r,r}+\frac{\kappa_r}{r}\}+A_{21}\{\varepsilon_{\theta m,r}+\frac{\varepsilon_{\theta m}}{r}\}+A_{22}\{\kappa_{\theta,r}+\frac{\kappa_\theta}{r}\}-A_{23}\{\phi_{,rr}+\frac{\phi_{,r}}{r}\}-A_{24}\{\phi_{,r}+\frac{\phi}{r}\} \\ &+A_{25}\kappa_r+A_{26}\kappa_\theta-A_{24}\phi_{,r}-A_{27}\phi=0 \end{aligned} \tag{18}$$

In this step, we can collect three essential equations for evaluation of the results of the problem. These equations include two mechanical equations and one electrical equation.

$$\frac{E_1}{1-\nu^2}\{\varepsilon_{rm,r}+\nu\varepsilon_{\theta m,r}\}+\frac{E_2}{1-\nu^2}\{\kappa_{rr,r}+\nu\kappa_{\theta\theta,r}\}+A_1\varepsilon_{rm,r}+A_2\kappa_{rr,r}+A_3\varepsilon_{\theta m,r}+A_4\kappa_{\theta\theta,r}+A_5\phi_{,rr}+A_6\phi_{,r}$$
$$\frac{E_1}{r(1+\nu)}\{\varepsilon_{rm}+\varepsilon_{\theta m}\}+\frac{E_2}{r(1+\nu)}\{\kappa_{rr}+\kappa_{\theta\theta}\}+\{A_1-A_3\}\frac{\varepsilon_{rm}}{r}+\{A_2-A_4\}\frac{\kappa_{rr}}{r}+\{A_3-A_7\}\frac{\varepsilon_{\theta m}}{r}+\{A_4-A_8\}\frac{\kappa_{\theta\theta}}{r}$$
$$+\{A_5-A_9\}\frac{\phi_{,r}}{r}+\{A_6-A_{10}\}\frac{\phi}{r}=0$$

$$\frac{E_2}{1-\nu^2}\{\varepsilon_{rm,r}+\nu\varepsilon_{\theta m,r}\}+\frac{E_3}{1-\nu^2}\{\kappa_{r,r}+\nu\kappa_{\theta,r}\}+A_2\varepsilon_{rm,r}+A_{11}\kappa_{r,r}+A_4\varepsilon_{\theta m,r}+A_{12}\kappa_{\theta,r}+A_{13}\phi_{,rr}+A_{14}\phi_{,r}$$
$$\frac{E_2}{r(1+\nu)}\{\varepsilon_{rm}+\varepsilon_{\theta m}\}+\frac{E_3}{r(1+\nu)}\{\kappa_r+\kappa_\theta\}+\{A_2-A_4\}\frac{\varepsilon_{rm}}{r}+\{A_{11}-A_{15}\}\frac{\kappa_r}{r}+\{A_4-A_8\}\frac{\varepsilon_{\theta m}}{r}+\{A_{12}-A_{16}\}\frac{\kappa_\theta}{r}$$
$$+\{A_{13}-A_{17}\}\frac{\phi_{,r}}{r}+\{A_{14}-A_{18}\}\frac{\phi}{r}-rF_{r,cr}\left(\frac{\partial^2 w}{\partial r^2}+\frac{1}{r}\frac{\partial w}{\partial r}\right)=0 \tag{19}$$

$$A_{19}\{\varepsilon_{rm,r}+\frac{\varepsilon_{rm}}{r}\}+A_{20}\{\kappa_{r,r}+\frac{\kappa_r}{r}\}+A_{21}\{\varepsilon_{\theta m,r}+\frac{\varepsilon_{\theta m}}{r}\}+A_{22}\{\kappa_{\theta,r}+\frac{\kappa_\theta}{r}\}-A_{23}\{\phi_{,rr}+\frac{\phi_{,r}}{r}\}-A_{24}\{\phi_{,r}+\frac{\phi}{r}\}$$
$$+A_{25}\kappa_r+A_{26}\kappa_\theta-A_{24}\phi_{,r}-A_{27}\phi=0$$

By considering the displacement fields and electric potential as follows:

$$u=u_{mn}\sin(\frac{m\pi r}{a})\sin(\frac{n\pi r}{b}),w=w_{mn}\sin(\frac{m\pi r}{a})\sin(\frac{n\pi r}{b}),\phi=\phi_{mn}\sin(\frac{m\pi r}{a})\sin(\frac{n\pi r}{b}) \tag{20}$$

We can evaluate the results of the problem in terms of different geometrical and material properties. Before final evaluation of the results, the distribution of material properties must be defined.

3 RESULTS AND DISCUSSION

Before solution of the problem, it is appropriate to define the material properties for the FG and FGP layers. For FG layer, it is assumed that the bottom of the plate is steel and top of that is ceramic. Therefore the distribution of the material properties for FG layer is (Ebrahimi and Rastgo 2008):

$$E(z)=(E_c-E_m)(\frac{1}{2}+\frac{z}{2h_e})^n+E_m \qquad -h_e\le z\le h_e \tag{21}$$

where, $E(z=-h_e)=E_m$, $E(z=h_e)=E_c$, $2h_e$ is thickness of elastic solid section of the plate and n is the non-homogenous index of ceramic-metal section of the plate. Figure 1 show the distribution of modulus of elasticity along the thickness direction of the plate in terms of different values of non homogenous index.

The distribution of the mechanical and electrical properties for the two FGP layers can be supposed as a power function along the thickness direction as follows (Khoshgoftar et al 2009; Arefi and Rahimi, 2010):

$$E(z) = E_i \left(\frac{|z|}{h_e}\right)^n \qquad h_e < |z| \le h_e + h_p \tag{22}$$

where, E_i represents the value of the all mechanical and electrical components at $|z| = h_e$ and h_e is thickness of the piezoelectric section. Other numerical parameters are considered as:

$$E_c = 3.8\times10^{11}\, pa, E_m = 2\times10^{11}\, pa, E_{h_e} = 7.6\times10^{10}\, pa, e_{1h_e} = 0.35 VmN^{-1}, e_{2h_e} = -0.16 VmN^{-1}$$
$$\eta_{1h_e} = 9.03\times10^{-11} mN^{-1}, \eta_{2h_e} = 5.62\times10^{-11} mN^{-1}$$

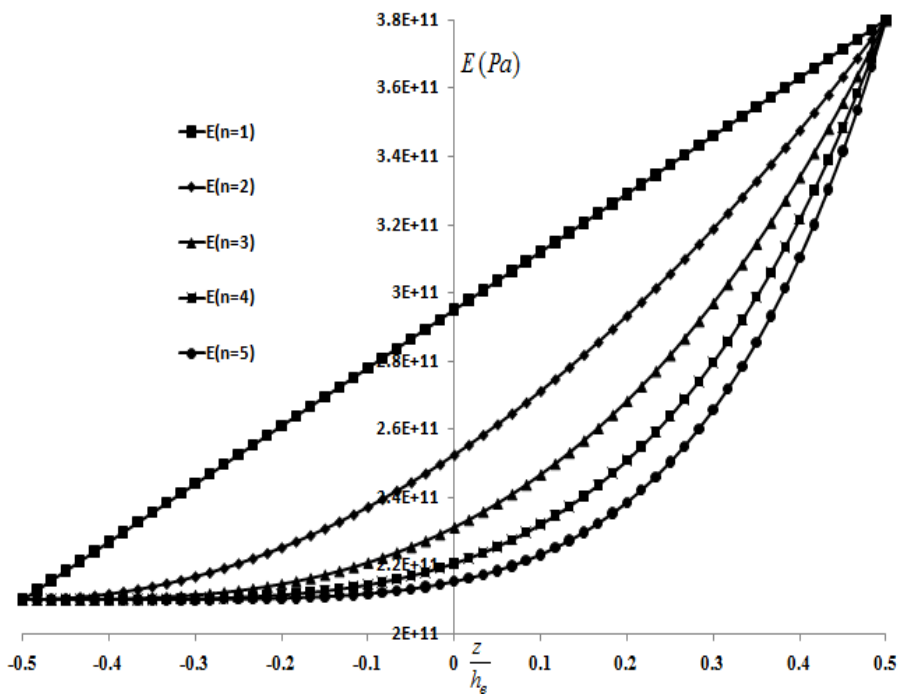

Figure 1: Distribution of variable modulus of elasticity of FGM along the thickness direction.

After defining the material properties, buckling load of FG circular plate integrated with piezoelectric layers can be evaluated. As a first case study, the effect of thickness of smart layers can be investigated on the buckling loads. For this study, three values of $\frac{h_e}{h_p}$ are considered.

Shown in figure 2 is the distribution of buckling load for different values of ratio of thickness $\frac{h_e}{h_p}$ in terms of non homogeneous index. The obtained results indicate that with increasing the ratio of thickness $\frac{h_e}{h_p}$, the buckling load of plate decrease. Shown in figure 3 is the distribution of buckling load for different values of outer radius of plate ($m = b/a$) in terms of non homogeneous index.

The obtained results indicate that with increasing the values of outer radius of plate ($m = b/a$), the buckling load doesn't obeying a uniform behavior. For selected values of outer radius ($m = 1.5, 2, 3$), it is observed that for increasing the value of m from 1.5 till 2, the buckling load increases and then with increasing the m from 2 till 3, the buckling load decreases.

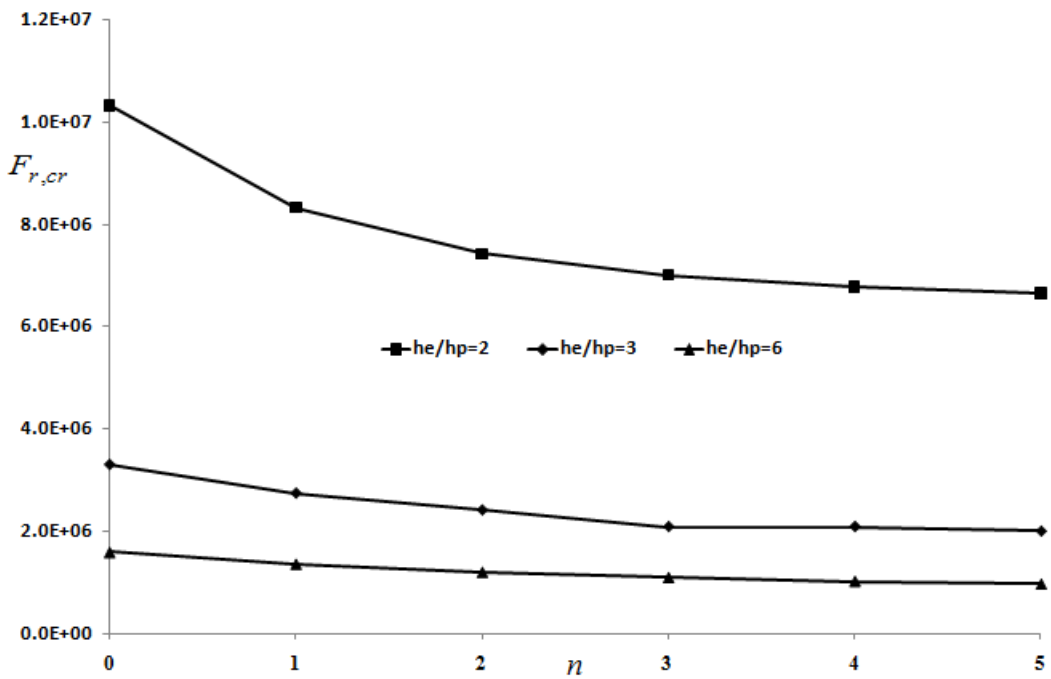

Figure 2: Buckling load of a FGP circular plate for of different values of piezoelectric thickness (h_e/h_p) in terms of non homogeneous index.

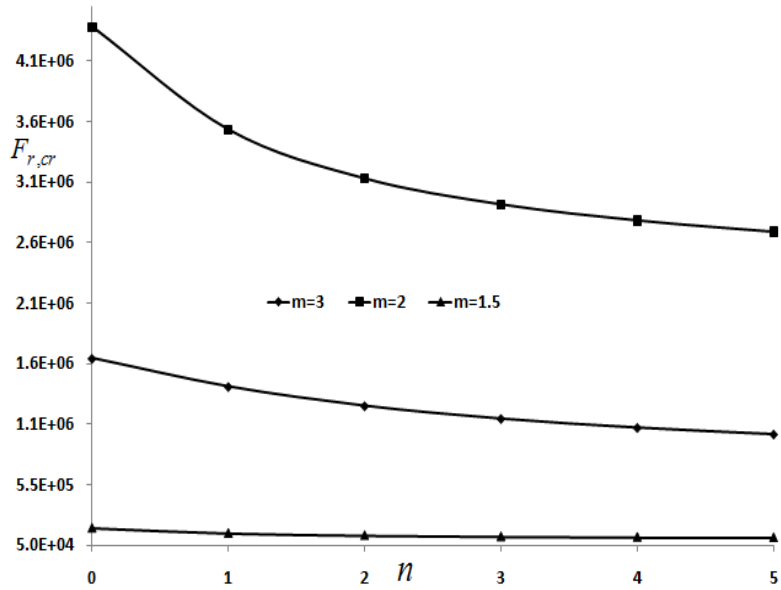

Figure 3: Buckling load of a FGP circular plate for different values of outer radius ($m = b/a$) in terms of non homogeneous index.

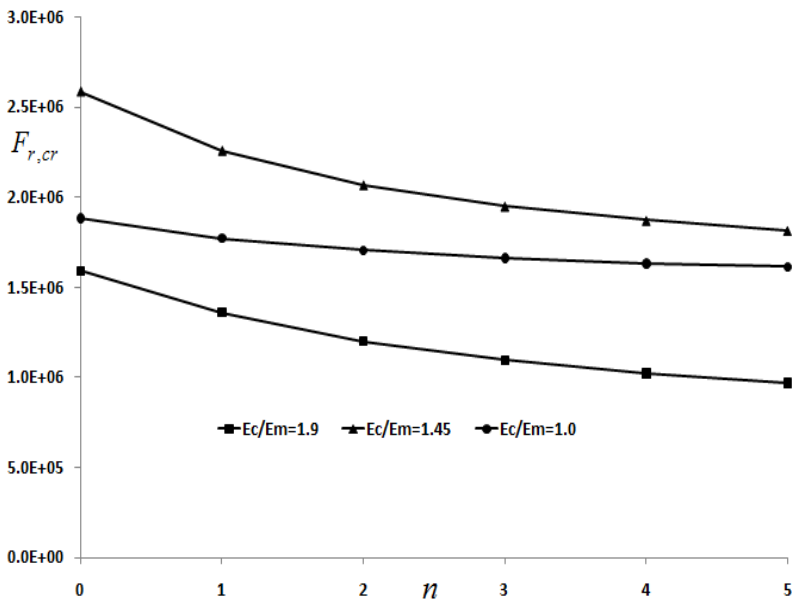

Figure 4: Buckling load of a FGP circular plate for different values of modulus elasticity of ceramic (E_c/E_m) in terms of non homogeneous index.

As another results of this research, the effect of stiffness of material can be considered on the results of the problem. This investigation can be performed by employing a dimensionless parameter such as (E_c/E_m). This study can be performed for three values of ($E_c/E_m = 1.9, 1.45, 1$) and in terms of various non homogenous index.

The obtained results in this figure indicate that the behavior of buckling load versus increasing or decreasing the ratio of modulus of elasticity (E_c/E_m) is not uniform. With increasing the E_c/E_m from 1 till 1.45, the buckling load increases and then with decreasing the E_c/E_m from 1.45 till 1.95, the buckling load decreases.

4 CONCLUSION

Electromechanical stability of a functionally graded circular plate integrated with two functionally graded piezoelectric layers under radial compressive load has been studied in this paper. All mechanical and electrical properties can be varied along the thickness direction. The effect of different geometrical and material parameters has been considered on the buckling load of the paper. The obtained results in this paper can direct engineers for production of electromechanical structures in technical application. This analysis shows that emploting a functionally graded material offers various options for optimized design. Evaluation of stability and buckling load is important for application of the piezoelectric structures in different conditions. The present results is applicable for engineer in fabrication of piezoelectric structures as electromechanical elements (sensor or actuator). Some important results are expressed as follows:

1. Investigation on the effect of ratio of thickness $\frac{h_e}{h_p}$ on the buckling load of circular plate indicates that with increasing the ratio of thickness $\frac{h_e}{h_p}$, the buckling load of plate uniformly decrease.

2. Investigation on the effect of outer radius of plate ($m = b/a$) indicates that the buckling load for increasing the value of m from 1.5 till 2 increases and then with increasing the m from 2 till 3, decreases. The same conclusion may be observed in studying the effect of the ratio of modulus of elasticity (E_c/E_m).With increasing the E_c/E_m from 1 till 1.45, the buckling load increases and then with decreasing the E_c/E_m from 1.45 till 1.95, the buckling load decreases

Acknowledgements

The authors would like to gratefully acknowledge the financial support by University of Kashan. Grant Number: 463865/02.

References

Arefi, M., Rahimi, G.H. (2010), Thermo elastic analysis of a functionally graded cylinder under internal pressure using first order shear deformation theory, Sci. Res. Essays, 5(12), 1442-1454.

Arefi, M., Rahimi, G.H. and Khoshgoftar, M.J. (2011), Optimized design of a cylinder under mechanical, magnetic and thermal loads as a sensor or actuator using a functionally graded piezomagnetic material, Int. J. Phys. Sci., 6(27): 6315-6322.

Arefi, M. and Rahimi, G.H. (2011a), Non linear analysis of a functionally graded square plate with two smart layers as sensor and actuator under normal pressure, Smart. Struct. Syst., 8(5): 433-446.

Arefi, M. and Rahimi, G.H. (2012b), Studying the nonlinear behavior of the functionally graded annular plates with piezoelectric layers as a sensor and actuator under normal pressure, Smart. Struct. Syst., 9(2): 127-143.

Arefi, M. and Rahimi, G.H. (2012c), Three-dimensional multi-field equations of a functionally graded piezoelectric thick shell with variable thickness, curvature and arbitrary nonhomogeneity, Acta. Mech., 223(3): 63-79.

Arefi, M., Rahimi, G.H. and Khoshgoftar, M.J. (2012d), Electro elastic analysis of a pressurized thick-walled functionally graded piezoelectric cylinder using the first order shear deformation theory and energy method, Mechanika., 18(3): 292-300.

Arefi, M., Rahimi, G.H. and Khoshgoftar, M.J. (2012e), Exact solution of a thick walled functionally graded piezoelectric cylinder under mechanical, thermal and electrical loads in the magnetic field, Smart. Struct. Syst., 9(5): 427-439.

Arefi, M., Rahimi, G.H. (2012f), The effect of nonhomogeneity and end supports on the thermo elastic behavior of a clamped-clamped FG cylinder under mechanical and thermal loads, Int. J. Pres. Ves. Piping. 96-97: 30-37.

Arefi, M., Rahimi, G.H. (2012g), Comprehensive thermoelastic analysis of a functionally graded cylinder with different boundary conditions under internal pressure using first order shear deformation theory, Mechanika, 18(1), 5-13.

Arefi, M. (2013), Nonlinear thermoelastic analysis of thick-walled functionally graded piezoelectric cylinder, Acta. Mech. 224, 2771–2783.

Mohammad Arefi, (2014), A complete set of equations for piezo-magneto-elastic analysis of a functionally graded thick shell of revolution, Latin American Journal of Solids and Structures 11 (11): 2073-2098.

Asemi, S.R, Farajpour, A., Borghei, M., Hassani, A.H., (2014), Thermal effects on the stability of circular graphene sheets via nonlocal continuum mechanics. Latin American Journal of Solids and Structures, 14(4): 704-724.

Arefi, M., Nahas, N., (2014), Nonlinear electro thermo elastic analysis of a thick spherical functionally graded piezoelectric shell, Compos Struct, 118, 510-518

Camier, C. Touzé, C. Thomas, O. (2009) Non-linear vibrations of imperfect free-edge circular plates and shells, Euro. J. Mech. A/Solids. 28: 500–515.

Ebrahimi, F. and Rastgo, A. (2008), An analytical study on the free vibration of smart circular thin FGM plate based on classical plate theory, Thin. Wall. Struct. 46 (12): 1402-1408.

Gaur, A. M., Rana, D. S. (2014), Shear Wave Propagation in Piezoelectric-Piezoelectric Composite layered structure, Lal. Am. J. Solids. Stru. 11 (13): 2483-2496.

Khoshgoftar, M.J. Ghorbanpour Arani, A. and Arefi, M. (2009), Thermoelastic analysis of a thick walled cylinder made of functionally graded piezoelectric material, Smart. Mater. Struct., 18 (11).

Kang, W. Lee, N-H. Pang, S. Chung, W. Y. (2005), Approximate closed form solutions for free vibration of polar orthotropic circular plates, Appl. Acoust. 66: 1162–1179.

Li, Q.S. Liu, J. Xiao, H.B. (2004) A new approach for bending analysis of thin circular plates with large deflection, Int. J. Mech. Sci. 46: 173–180

Ma, L.S. Wang, T.J. (2003). Nonlinear bending and post-buckling of a functionally graded circular plate under mechanical and thermal loadings, Int. J. Solids. Struct. 40: 3311–3330.

Nosier, A. Fallah, F. (2009) Non-linear analysis of functionally graded circular plates under asymmetric transverse loading, Int. J. Non-Linear Mech. 44: 928 – 942.

O¨ zakc, M. Tays, N. Kolcu, i, F. (2003), Buckling analysis and shape optimization of elastic variable thickness circular and annular plates—II. Shape optimization, Eng. Struct. 25: 193–199.

Rahimi, G.H. Arefi, M. and Khoshgoftar, M.J. (2011), Application and analysis of functionally graded piezoelectrical rotating cylinder as mechanical sensor subjected to pressure and thermal loads , Appl. Math. Mech.-Eng., 32 (8): 997-1008.

Sahraee, S. Saidi, A.R. (2009) Axisymmetric bending analysis of thick functionally graded circular plates using fourth-order shear deformation theory, Euro. J. Mech. A/Solids. 28: 974–984

Saidi, A.R. Rasouli, A. Sahraee, S. (2009) Axisymmetric bending and buckling analysis of thick functionally graded circular plates using unconstrained third-order shear deformation plate theory, Compos. Struct. 89: 110–119

Sekouri, E. M. Hu, Y. R. Dung Ngo, A. (2004) Modeling of a circular plate with piezoelectric actuators, Mechatronics. 14: 1007–1020.

Tylikowski, A. Frischmuth, K. (2003) Stability and stabilization of circular plate parametric vibrations, Int. J. Solids. Struct. 40: 5187–5196

Vivio, F. Vullo, V. (2010). Closed form solutions of axisymmetric bending of circular plates having non-linear variable thickness, Int. J. Mech. Sci. 52: 1234–1252.

Wu, T.Y. Wang, Y.Y. Liu, G.R. (2002). Free vibration analysis of circular plates using generalized differential quadrature rule, Comput. Methods. Appl. Mech. Engrg. 191: 5365–5380

Yalcin, H. S. Arikoglu, A. Ozkol, I. (2009) Free vibration analysis of circular plates by differential transformation method, Appl. Math. Comput. 212: 377–386.

Zhou, D. Au, F.T.K. Cheung, Y.K. Lo, S.H. (2003) Three-dimensional vibration analysis of circular and annular plates via the Chebyshev–Ritz method, Int. J. Solids. Struct. 40: 3089–3105.

Appendix A

$$E_1=\int_{-h_e}^{h_e}E(z)dz\,,E_2=\int_{-h_e}^{h_e}zE(z)dz\,,E_3=\int_{-h_e}^{h_e}z^2E(z)dz$$

$$A_1=2\int_{h_e}^{h_e+h_p}C^p{}_{rrrr}(z)dz\,,A_2=2\int_{h_e}^{h_e+h_p}zC^p{}_{rrrr}(z)dz\,,A_3=2\int_{h_e}^{h_e+h_p}C^p{}_{rr\theta\theta}(z)dz\,,A_4=2\int_{h_e}^{h_e+h_p}zC^p{}_{rr\theta\theta}(z)dz$$

$$A_5=2\int_{h_e}^{h_e+h_p}e_{rrr}f(z)dz\,,A_6=2\int_{h_e}^{h_e+h_p}e_{rrz}f_{,z}(z)dz\,,A_7=2\int_{h_e}^{h_e+h_p}C^p{}_{\theta\theta\theta\theta}(z)dz\,,A_8=2\int_{h_e}^{h_e+h_p}zC^p{}_{\theta\theta\theta\theta}(z)dz$$

$$A_9=2\int_{h_e}^{h_e+h_p}e_{\theta\theta r}f(z)dz\,,A_{10}=2\int_{h_e}^{h_e+h_p}e_{\theta\theta z}f_{,z}(z)dz\,,,A_{11}=2\int_{h_e}^{h_e+h_p}z^2C^p{}_{rrrr}(z)dz\,,A_{12}=2\int_{h_e}^{h_e+h_p}z^2C^p{}_{rr\theta\theta}(z)dz$$

$$A_{13}=2\int_{h_e}^{h_e+h_p}ze_{rrr}f(z)dz\,,A_{14}=2\int_{h_e}^{h_e+h_p}ze_{rrz}f_{,z}(z)dz\,,A_{15}=2\int_{h_e}^{h_e+h_p}z^2C^p{}_{\theta\theta rr}(z)dz\,,A_{16}=2\int_{h_e}^{h_e+h_p}z^2C^p{}_{\theta\theta\theta\theta}(z)dz$$

$$A_{17}=2\int_{h_e}^{h_e+h_p}e_{\theta\theta r}f(z)dz\,,A_{18}=2\int_{h_e}^{h_e+h_p}e_{\theta\theta z}f_{,z}(z)dz\,,A_{19}=2\int_{h_e}^{h_e+h_p}e_{rrr}(z)dz\,,A_{20}=2\int_{h_e}^{h_e+h_p}ze_{rrr}(z)dz$$

$$A_{21}=2\int_{h_e}^{h_e+h_p}e_{r\theta\theta}(z)dz\,,A_{22}=2\int_{h_e}^{h_e+h_p}ze_{r\theta\theta}(z)dz\,,A_{23}=2\int_{h_e}^{h_e+h_p}\eta_{rr}f(z)dz\,,A_{24}=2\int_{h_e}^{h_e+h_p}\eta_{rz}f_{,z}(z)dz$$

$$A_{25}=2\int_{h_e}^{h_e+h_p}e_{zrr}(z)dz\,,A_{26}=2\int_{h_e}^{h_e+h_p}e_{z\theta\theta}(z)dz\,,A_{27}=2\int_{h_e}^{h_e+h_p}\eta_{zz}(z)f_{,zz}dz$$